biomechanics

Article

Kinematic Analysis of the Temporomandibular Joints for Different Head Positions—A Reliability Study

Gaël Bescond [1,2,*], Céline De Passe [3], Véronique Feipel [1,2,4], Joe Abi Nader [2,4], Fedor Moiseev [1] and Serge Van Sint Jan [1,2]

[1] Laboratory of Anatomy, Biomechanics and Organogenesis (LABO), Faculty of Medicine, Université Libre de Bruxelles (ULB), 1070 Bruxelles, Belgium; veronique.feipel@ulb.be (V.F.); fedor.moiseev@framasoft.com (F.M.); serge.van.sint.jan@ulb.be (S.V.S.J.)
[2] Center for Functional Evaluation (CFE), Faculty of Medicine, Université Libre de Bruxelles (ULB), 1070 Bruxelles, Belgium; joe.abi.nader@ulb.be
[3] Department of Dentistry, Oral and Maxillo-Facial Surgery, Ortho Dentistry and Stomatology, Erasme Hospital, Faculty of Medicine, Université Libre de Bruxelles (ULB), 1070 Bruxelles, Belgium; celine.de.passe@ulb.be
[4] Laboratory of Functional Anatomy (LAF), Faculty of Motor Sciences, Université Libre de Bruxelles (ULB), 1070 Bruxelles, Belgium
* Correspondence: gael.bescond@ulb.be; Tel.: +32-2-555-6379

Abstract

Background/Objectives: Considering that the kinematics of the temporomandibular joints (TMJs) is concomitant with head movements and that temporomandibular joint disorders (TMDs) are frequently associated with neck pain in clinics but seldom or never investigated, the aim of this study was to develop a reliable in vivo measurement protocol of the simultaneous amplitudes of the mandible and of the skull. The development of such a protocol is part of a project to build an accurate kinematic assessment tool for clinicians in the orofacial field who treat patients suffering from TMD. **Methods**: Mouth opening, laterotrusion and protrusion movements for three different positions of the head (neutral, slouched and military) on 12 asymptomatic voluntary subjects (5 men and 7 women, mean 33.6 yo +/− 11.1) were recorded using 20 markers palpated and taped and 14 optoelectronic cameras. The acquisition frequency was set at 150 hertz. The inter- and intra-examiner reliability of marker palpation in mm was calculated using standard deviation (SD), mean difference (MD) and standard error (SE). Amplitudes of movement according to axes defined by the International Society of Biomechanics (ISB) are given for the mandible and skull segments. The propagation of error on the amplitudes was calculated with the root mean square propagation error (RMSPE) in degrees. Repeated-measures ANOVA or Friedman tests were used to assess the influence of the position of the head on the amplitudes of the jaw. Power analysis of the sample size was estimated with Cohen's f3 size effect test. Steady-state plots (SSPs) and normalized motion graphs between the skull and the mandible motion were performed to study the coordination of their maximum amplitude over time. **Results**: The protocol demonstrated good intra-examiner reliability ($1.5 < MD < 5.8$; $2.6 < SD < 7.8$; $2.0 < SE < 3.8$), good inter-examiner reproducibility ($0.2 < MD < 4.0$; $3.5 < SD < 4.6$; $2.0 < SE < 2.5$) and small error propagation ($0.0 < RMSPE\ intra < 2.8$; $0.0 < RMSPE\ inter < 1.0$). The amplitudes of the jaw and head found during the three types of movements correspond to the values reported in the literature. Head positions did not appear to significantly influence the amplitudes of jaw movements, which could be explained by the power estimation of our sample (Type II error $\beta = 0.692$). The participation of head movements in those of the jaw, for all motions and in all positions, was demonstrated and discussed in detail. **Conclusions**: The accuracy, test–retest reliability, and intra-individual variability of the TMJ kinematic analysis, including head movements, was ensured. The small sample size

Check for updates

Academic Editor: Tibor Hortobágyi

Received: 16 October 2025
Revised: 3 January 2026
Accepted: 6 January 2026
Published: 10 January 2026

Copyright: © 2026 by the authors. Licensee MDPI, Basel, Switzerland. This article is an open access article distributed under the terms and conditions of the Creative Commons Attribution (CC BY) license.

and the absence of standardized head positions for the subjects limit the scope of the intra- and inter-group analysis results. Given the natural biological and complex coordination of jaw–head movement, the authors consider its evaluation useful in clinical intervention and would like to further develop the present protocol. The next step should be to test the feasibility of its clinical application with a larger group of asymptomatic subjects compared to patients suffering from TMD.

Keywords: kinematics; temporomandibular joint; head position; anatomical landmarks; anatomical frames; motion analysis; reliability; motion capture; error propagation

1. Introduction

Among the factors influencing the kinematics of the temporomandibular joint (TMJ), chronic neck pain is recognized as being able to modify the TMJ range of movement [1,2]. Also, some patients suffering from temporomandibular disorders (TMDs) describe secondary pain in the cervical region [3,4].

It has been shown that, in a static situation and for a different head position in space, a change in the resting mandibular position and, therefore, in interdental contacts are observed. Indeed, occlusal contacts of the dental arches occur anteriorly when the head is tilted forward (cervical spine in flexion). Conversely, occlusal contacts occur more posteriorly when the head is tilted backwards (cervical spine in extension) [5].

Some authors hypothesized that occlusion, and therefore dental class, influences cervical posture: Class II patients tend to flex their cervical spine, while Class III patients tend to extend it [6]. Normalization of occlusion (by orthognathic surgery) could lead to normalization of posture [7].

Without going as far as these authors, who assert a causal link that is strongly challenged by others [8], the literature nonetheless suggests an epidemiological link. As mentioned above, neck pain is a symptom regularly associated with TMD which is explained in various ways by different authors. The anatomical continuity between the masticatory and cervical muscles via the hyoid bone constitutes a first causal hypothesis [1]. The hyoid muscles stabilize the hyoid bone during mouth opening, allowing the digastric muscle to perform its role of lowering the mandible [9]. A second hypothesis explains the association between cervical and TMJ symptoms by the convergence of cervical and trigeminal nociceptive pathways at the trigeminal-cervical nucleus [10]. Finally, a third hypothesis describes a vicious circle, where pain impedes normal muscle function and leads to increased pain [11].

Our study does not claim to investigate either of these causal hypotheses. However, this review highlights the need to develop a common protocol for kinematic analysis of the jaw and cervical spine.

Several kinematic studies have observed that changes in the posture of the head influence the amplitude of mouth opening. In 1984, Goldstein et al. used a kinesiograph to demonstrate changes in the vertical and anterior-posterior trajectories of the mandible during mouth opening movements depending on the initial position of the head [12]. In 2000, Visscher et al. observed changes in the trajectory of the incisors during mouth opening in five different head positions, using an optoelectronic motion capture system [13], and Zafar et al. highlighted the improvement in temporal coordination between mandibular and cranial movements with increased mouth opening speed [14]. Eriksson et al. studied variations in the amplitude of head extension during rhythmic mandibular opening movements and observed a significant decrease in amplitude during unilateral chewing [15].

More recently, Prodoehl et al., in a quantified kinematic study, showed the influence of the starting position on the amplitude of movement of the head relative to the thorax during maximum mouth opening [16], and Nilsson et al. established the accuracy and validity of a protocol for measuring mandibular movements in terms of volume and area, without however evaluating those of the cervical spine [17].

While highlighting the long-standing functional links (dating back to fetal yawning [14]) between the jaw and the cervical spine, kinematic analysis protocols either failed to quantify head movements in relation to the thorax [12–14,17] or had not been subjected to validity and accuracy tests [12–16].

Therefore, the aim of this study is to develop a protocol for measuring the amplitudes of simultaneous movements of the mandible compared to the skull and of the skull compared to the thorax, during mouth opening and closing, protrusion and laterotrusion, for healthy subjects. By quantifying head movements relative to the thorax, we explore the indirect contribution of the cervical spine during TMJ movements and study the temporal coordination between mandibular and cervical kinematics. We also investigate the reliability of the protocol (in terms of reproducibility and error propagation) in order to test its feasibility and applicability, and eventually to propose it in a clinical evaluation context.

2. Materials and Methods

2.1. Population Recruitment and Preparation

Twelve subjects (5 men and 7 women) aged between 19 and 57 years (mean 33.6 yo +/− 11.1) were recruited on a voluntary basis, informed of the benefits and risks associated with the experimental procedures and signed a written informed consent form approved by the Board of Ethics of the Université Libre de Bruxelles (ULB) (No. SRB2023/356). They answered an evaluation questionnaire based on the Recommendations and Diagnostic Criteria for Temporomandibular Disorders (RDC-TMD) [18] and the Craniocervical Dysfunction Index (CCDI) [19] to exclude the presence of pathologies or history at the cervical level, TMJs, or masticatory muscles. A clinical examination consisting of the head and neck palpation, caliper measurement of the amplitudes of movement of opening, laterotrusion and protrusion of the mandible, and verification of non-painful cervical movements was also carried out by a stomatologist.

To begin with, a lower dental arch print was taken from subjects included in the study with alginate, based on standard clinical procedures, in the Hôpital Universitaire de Bruxelles. The questionnaire, functional and palpatory examination, and mandibular dental arch print did not exceed 15 min per subject.

From the plaster model, a personalized dental splint in thermoformed resin was made, with a tip to attach four reflective markers (Jaw cluster with four markers—Jaw 1, Jaw 2, Jaw 3, Jaw 4—rigidly attached to it) to the inter-incisal area, on the vestibular side (Figure 1).

The splint was not actually screwed into the subject's jaw. Nevertheless, as it was completely adherent to the subject's teeth and the rods connecting the splint to the markers were made of metal, it was considered that the relationship between the cluster and the mandible was rigid, as used in the study by Prodoehl et al. [16].

During a second appointment in the ULB Center for Functional Evaluation, the same examiner palpated 11 anatomical landmarks (ALs) (Table 1) on the head and thorax of each subject to place self-reflecting markers used to construct anatomical frames (AFs), one for each segment of interest. The overall time required to palpate the 11 ALs was less than 10 min on average.



(**a**) (**b**) (**c**)

Figure 1. (**a**) Dental arch print in alginate; (**b**) personalized dental splint on the plaster model (the splint is transparent and covers the entire dental arch to ensure stability); (**c**) personalized dental splint with the jaw cluster fixed on it.

Table 1. Anatomical Landmarks (ALs) palpated and glued on the subjects. In green, ALs palpated on the skull. In blue, ALs palpated on the thorax. In purple, ALs on the cluster of the mandible.

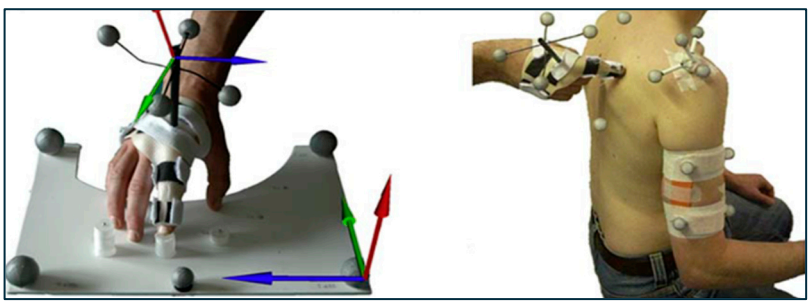
LTRAG	Left tragus	LAT	Left acromial tip	JAW 1
RTRAG	Right tragus	RAT	Right acromial tip	JAW 2
LIOF	Left infraorbital foramen	JN	Jugular notch	JAW 3
RIOF	Right infraorbital foramen	TH2	Spinous process of TH2	JAW 3
LZA	Left zygomatic angle			
RZA	Right zygomatic angle			
GL	Glabella			

The markers palpated and placed on the subject's head were defined using observable ALs, chosen so that they were relatively easy to identify by palpation and their determination was repeatable (Table 1). Also, as they did not cover any significant soft tissue, we therefore did not consider skin deformation during movement.

Then, the subject placed the dental splint in their mouth equipped with the four ALs (JAW 1, 2, 3, 4) and sat straight on a stool, looking towards a target at eye level so the gaze was horizontal.

2.2. Motion Data Collection

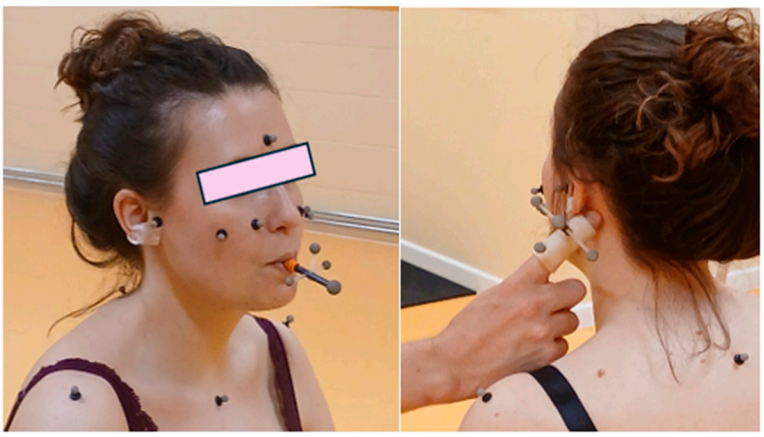
Another manual palpation was performed using an anatomical palpation device outfitted with a cluster: the A-Palp (Figure 2) [20].



(**a**) (**b**)

Figure 2. (**a**) Gantlet and finger pulp calibration. The arrows define the anatomical frames of the A-Palp and the calibration board.; (**b**) AL static calibration (20).

The index pulp directly located a succession of five additional ALs on the subject's head and mandible, landmarks on which a marker could not be glued (Figure 3 and Table 2 for a detailed list of the supplementary palpated ALs).



(**a**) (**b**)

Figure 3. (**a**) Subject sitting straight on the stool, looking forward, with the personalized dental splint in the mouth and self-reflecting markers on Als. (**b**) Examiner performing palpation with the A-Palp on 5 supplementary Anatomical Landmarks, here the left mastoid process.

Table 2. Supplementary ALs palpated with the A-Palp on the subjects. In green, ALs palpated on the skull. In purple, ALs palpated on the mandible.

RMP	Right mastoid process	MP	Mental protuberance
LMP	Left mastoid process	RAN	Right gonion
		LAN	Left gonion

This palpation followed strict guidelines [21]. The instantaneous position of each of the 5 ALs was digitized into 5 standard C3D files, using a standard stereophotogrammetric system with 14 cameras (Vicon© Nexus Vicon Motion Systems Ltd. Oxford Metrics. Oxford. UK). Sampling frequency was set at 150 Hz.

The positions of the markers palpated using the A-Palp on the subject's head were recorded by the optoelectronic system, so skin artefacts that could cause wobbling were again not considered.

The subject, still seated on the stool and looking straight ahead towards a target to keep the gaze horizontal, initially kept their mouth closed with the mouthpiece in place. This static position in maximal occlusion was maintained for a few seconds at the start of each recording in order to establish a standardized starting position.

Then, each subject performed a series of 10 repetitions of 3 different movements at a comfortable self-selected speed: (1) 10 mouth opening and closing cycles at maximum amplitude, (2) 10 left and right laterotrusions at maximal amplitude (i.e., lateral excursions, beginning with the left), (3) 10 protrusions at maximal amplitude.

They performed the movements in 3 different cervical spine attitudes: (1) neutral, i.e., comfortable and free, (2) slouched, i.e., with the back relaxed, the shoulders hanging forward and the head bent slightly over, (3) in the military position, i.e., with the back very straight and stiff.

We did not reject any recordings and processed all the data obtained during all the trials.

During these movements, the trajectory of the markers and clusters of landmarks was recorded by cameras, and each motion was stored in standard C3D files, subsequently imported into the lhpFusionBox software (Version number 20240925), a musculoskeletal data fusion software developed at ULB during previous European-funded projects from open-source libraries [22].

2.3. Anatomical Frames Construction

The International Society of Biomechanics (ISB) recommendations [23,24] were respected in order to build and orient anatomical frames (AFs). Since the literature does not describe AFs specific to the mandible, we constructed them based on the markers palpated and recorded in the lhpFusionBox software. We used 3 landmarks (P1, P2, P3) with the *Z*-axis kept aligned between 2 landmarks (P1, P2) and applied the following mathematical definition to build the frames.

The first axis Z (displayed in blue) was constructed between P1 and P2 as a normalized vector difference between P1 and P2: $\vec{Z} = \frac{P_2 - P_1}{\|P_2 - P_1\|}$.

By default, the origin (O) of the system was the middle of P1 and P2: $O = \frac{P_1 + P_2}{2}$.

Then, a vector O-P3 was built: $\vec{Y}_{aux} = \frac{P_3 - O}{\|P_3 - O\|}$.

Then, a second axis X (displayed in red) takes the cross product between Z and $\vec{Y}_{aux}$: $\vec{X} = \frac{\vec{Z} \times \vec{Y}_{aux}}{\left\| \vec{Z} \times \vec{Y}_{aux} \right\|}$.

Finally, Y (displayed in green) was found from the cross product between X and Z: $\vec{Y} = \frac{\vec{X} \times \vec{Z}}{\left\| \vec{X} \times \vec{Z} \right\|}$.

Thus, two coordinate systems were built: a Jaw Global Frame (JGF) associated with a Skull Global Frame (SGF), and a Thorax Global Frame (TGF) associated with the SGF (Figure 4).

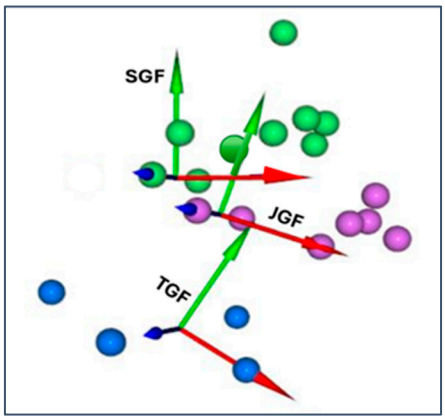


Figure 4. Screen shot of a right lateral view of the ALs and AFs built in LhpFusionBox. Green balls: skull Anatomical Landmarks (ALs), SGF: Skull Global Frame. Purple balls: jaw ALs, JGF: Jaw Global Frame. Blue balls: thorax ALs, TGF: Thorax Global Frame.

2.3.1. Construction of the JGF

The *Z*-axis (blue) was defined between the Left and the Right Jaw Angles (LJA and RJA) with the JGF origin located on the midpoint between both ALs; the *Z*-axis was oriented towards the right of the bone of interest. The *Z*-axis and the Mental Protuberance (MP) allowed the construction of a virtual plane close to the anatomical horizontal plane. The *Y*-axis (green) was then obtained orthogonally to this plane and ran upwards through the JGF origin. The *X*-axis (red) was obtained as the cross-product of the *Z*- and *Y*-axis. Since it

was pointing downward, we rotated all JGF and for all subjects around the *Z*-axis by 90° to make it point forward. The JGF was then aligned with the body of the jaw.

2.3.2. Construction of the SGF

The *Z*-axis (blue) was defined between the Left and the Right Mastoid Processes (LMP and RMP), oriented towards the right of the bone of interest. We then proceeded to the cross-product between the *Z*-axis and a virtual plane oriented towards the Glabella (GL) to obtain an orthogonal axis to the *Z*-axis: the *Y*-axis (green) oriented towards the front and the top. The *X*-axis (red) was calculated as the cross-product between the Z- and *Y*-axis. The *X*-axis was oriented towards the front and the bottom, so we rotated all SGF and for all subjects 35° around the *Z*-axis to align it with the JGF.

2.3.3. Construction of the TGF

The *Z*-axis (blue) was defined between LAT and RAT, oriented towards the right. We then proceeded to the cross-product between the *Z*-axis and a virtual plane oriented towards the Jugular Notch (JN) to obtain an orthogonal axis to the *Z*-axis: the *Y*-axis (green) oriented towards the front and the top. The *X*-axis (red) was calculated as the cross-product between the Z- and *Y*-axis. The *X*-axis was pointing downwards, so a 90° rotation around the *Z*-axis was performed for all TGF and for all subjects to align the *X*-axis with the SGF. The TGF was then also aligned with the skeletal upper opening of the thorax (between the acromions, the second thoracic vertebra and the jugular notch).

2.4. Data Fusion

Spatio-temporal fusion of ALs and kinematic data consisted of a process previously implemented in the lhpFusionBox through a batch procedure [25–27]. It consisted of registering all 20 manually palpated and glued ALs (Tables 1 and 2) with the 3 recorded motions (mouth opening and closing, laterotrusion and protrusion). This led to the fusion of all AL coordinates with the C3D motion files into one unique data structure.

Orientation of Vector Position motion graphs (including rotations on X-, Y- and Z- axes and translations along X-, Y- and Z-axes) were obtained for all 3 motions (mouth opening and closing, laterotrusion and protrusion) collected from the 12 subjects and smoothed using cubic spline filtering [28].

We chose cubic spline smoothing as it has been demonstrated to effectively enable the removal of high-frequency noise as well as stable analytical derivatives of velocity and acceleration, which are very useful quantities for kinematic studies [29]. Also, with splines it is possible to process data with unequal sampling intervals, and the boundary conditions will stay well-defined [30].

With an acquisition frequency of 150 Hz, we set the smoothing to 0.0005, as recommended to obtain optimal moderate smoothing for movement data between 100 and 200 Hz, with an expected noise level of 1 to 2 mm [24].

A custom-made Matlab® procedure was used (Matlab Version number R2017b, from MathWorks, Inc.) to normalize the 10 cycles of motion into one normalized motion expressed from 0 to 100%. We applied this averaging on the second to ninth motion to avoid potential bias such as the subject only beginning to move during the first movement or slowing down during the last. Averaging, while eliminating the variability in range of motion for each subject, is useful for facilitating comparisons between subjects, while retaining the extreme values expressed in the standard deviations.

2.5. Statistical Analysis

Three different examiners palpated ALs on 3 occasions, one week apart so that a reliability analysis of the AL palpation could be performed. Mean differences and standard deviation were calculated to determine dispersion of values and standard error to extend it to a population [31]. The Wilcoxon signed rank test was used to identify the most accurately reproduced ALs between those taped and those palpated with the A-Palp. The root mean square propagation error was used to investigate the propagation of AL palpation error onto the range of motions, as well as the mean differences between them, with a confidence interval set at 95%.

Also, descriptive statistics investigated the amplitudes of the 3 different movements in the 3 different positions. Normality of distribution was verified by Q-Q plots.

To test whether the position of the head influences the amplitudes of movement within the TMJ, repeated-measures ANOVA or a Friedman test for non-parametric data were used. In the event of significant results, it was planned to submit the mean values to Tukey's post hoc tests.

A power estimation analysis was also carried out using the collected data to check whether statistical conclusions could be validated despite the small size of the sample (n = 12) with a Cohen's f3 effect size test [32].

To evaluate the contribution of head movements during jaw movements, the coefficient determination of these two variables was calculated, as well as the percentage of the head contribution during the movements of the jaw. Steady-state plots and normalized motion graphs between the main components of the skull and the mandible motion were performed to study their coordination and maximum amplitude over time.

3. Results

3.1. Reliability Study

Table 3 provides the mean difference (MD), standard deviation (SD), and standard error (SE) in mm for all technical-glued ALs and those palpated with the A-Palp ALs.

Table 3. Intra- and inter-examiner reliability on the spatial location of palpated ALs, according to Jaw Global Frame, Skull Global Frame or Thorax Global Frame. Mean difference (MD), standard deviation (SD) and standard error (SE) in mm. Palpated ALs with the A-Palp device are in **bold**.

	Intra-Examiner									**Inter-examiner**		
	Examiner A			**Examiner B**			**Examiner C**					
ALs	**MD**	**SD**	**SE**	**MD**	**SD**	**SE**	**MD**	**SD**	**SE**	**MD**	**SD**	**SE**
Jaw1	0.4	1.8	0.9	−4.2	2.3	1.2	0.0	0.1	0.0	−1.3	2.5	1.3
Jaw2	−0.2	2.2	1.1	−3.1	1.4	0.9	−0.1	1.2	0.6	−1.1	1.7	1.0
Jaw3	−0.2	2.5	1.4	−2.7	2.3	1.3	−0.4	1.9	1.2	−1.1	1.4	1.0
Jaw4	−0.7	1.3	0.9	−3.7	1.8	0.9	−0.6	0.8	0.3	−1.6	1.7	1.0
GL	−0.1	11.3	6.3	3.8	1.7	1.0	−1.5	0.6	0.3	0.7	2.7	1.5
RIOF	1.7	11.7	6.6	−4.3	2.6	1.5	−2.7	1.9	1.0	−1.8	3.1	1.9
RZA	1.6	5.9	3.5	−2.6	4.5	2.4	−1.1	3.6	2.1	−0.7	2.1	1.4
RTRAG	−1.1	1.7	1.0	−2.7	7.4	4.1	−2.5	1.1	0.9	−2.1	0.8	0.6
LIOF	−0.5	14.5	8.4	−2.5	1.1	0.7	−1.5	0.7	0.3	−1.5	1.0	0.6
LZA	−0.6	9.9	5.5	−0.3	1.7	0.9	−0.2	0.2	0.0	−0.4	0.2	0.3
LTRAG	−2.9	2.3	1.3	−0.8	0.4	0.3	−2.6	3.6	1.9	−2.1	1.1	0.7

Table 3. *Cont.*

	Intra-Examiner									Inter-examiner		
	Examiner A			Examiner B			Examiner C					
ALs	**MD**	**SD**	**SE**	**MD**	**SD**	**SE**	**MD**	**SD**	**SE**	**MD**	**SD**	**SE**
JN	1.2	5.4	2.9	−3.0	1.7	1.1	−5.2	5.4	3.2	−2.3	3.3	1.8
LAT	−7.3	6.9	4.2	−9.0	5.2	2.3	−20.3	12.7	7.2	−12.2	7.1	4.0
RAT	−0.8	1.8	0.9	−5.2	7.4	4.3	−4.3	3.5	2.0	−3.4	2.3	1.2
TH2	−12.6	21.8	12.8	−26.7	12.4	7.3	−22.7	16.0	9.4	−20.7	7.2	4.2
RJA	0.9	1.2	0.9	2.5	2.6	1.3	−2.9	1.4	0.6	0.1	2.8	1.5
MP	−0.4	5.8	3.5	−3.3	1.8	1.2	2.4	1.0	0.7	−0.5	2.9	1.4
LJA	−2.4	4.5	2.7	3.7	3.9	2.2	−1.0	2.8	1.8	0.1	3.2	1.9
LMP	1.1	3.8	2.3	14.0	23.6	13.5	−0.5	1.4	0.9	4.9	8.0	4.7
RMP	5.3	18.7	11.1	−0.4	5.3	3.2	−4.4	1.9	1.3	0.1	4.9	2.6
Mean	−0.9	6.8	3.0	−2.5	4.6	2.6	−3.6	3.1	1.8	−2.3	3.0	1.7

The Wilcoxon signed rank test, with a *p*-value of 0.125, highlighted the greater precision of markers palpated with the A-Palp compared with glued markers.

From the opening/closing motion, we calculated the intra- and inter-examiner Root Mean Square Propagation Error (RMSPE), the mean differences with a confidence interval set at 95%, for the jaw displacement around the SGF Z-, X- and Y- axes, and the skull displacement around the TGF Z-, X- and Y- axes, as shown in Table 4.

Table 4. Inter and intra-examiner Root Mean Square Palpation Error (RMSPE), Mean Difference (MD) with a Confidence Interval set at 95% [CI 95%] between the kinematic data for the mandible and the skull rotation around respectively the Z-, X- and Y- axes of the Skull Global Frame (SGF), and Z-, X- and Y- axes of the Thorax Global Frame (TGF) (in degrees).

Rot Z Jaw in SGF	Inter		Intra					
			Exam 1		Exam 2		Exam 3	
	RMSPE	MD [CI 95%]	RMSPE	MD [CI 95%]	RMSPE	MD [CI 95%]	RMSPE	MD [CI 95%]
	1.0	1.0 [0.9; 1.2]	2.1	2.2 [1.9; 2.5]	2.8	2.8 [2.4; 3.1]	0.9	0.2 [0.2; 02]
Rot Z Skull in TGF	Inter		Intra					
			Exam 1		Exam 2		Exam 3	
	RMSPE	MD [CI 95%]	RMSPE	MD [CI 95%]	RMSPE	MD [CI 95%]	RMSPE	MD [CI 95%]
	0.2	0.2 [0.2; 0.2]	0.3	0.3 [0.3; 0.3]	0.0	0.3 [0.3; 0.3]	0.3	0.7 [0.6; 0.8]
Rot X Jaw in SGF	Inter		Intra					
			Exam 1		Exam 2		Exam 3	
	RMSPE	MD [CI 95%]	RMSPE	MD [CI 95%]	RMSPE	MD [CI 95%]	RMSPE	MD [CI 95%]
	0.0	0.4 [0.3; 0.4]	0.1	0.2 [0.1; 0.2]	0.4	1.0 [0.8; 1.1]	0.1	0.3 [0.2; 0.3]
Rot X Skull in TGF	Inter		Intra					
			Exam 1		Exam 2		Exam 3	
	RMSPE	MD [CI 95%]	RMSPE	MD [CI 95%]	RMSPE	MD [CI 95%]	RMSPE	MD [CI 95%]
	0.0	0.2 [0.1; 0.2]	0.0	0.2 [0.1; 0.2]	0.1	0.2 [0.1; 0.2]	0.0	0.1 [0.1; 0.1]

Table 4. *Cont.*

Rot Y Jaw in SGF	Inter		Intra					
			Exam 1		Exam 2		Exam 3	
	RMSPE	MD [CI 95%]	RMSPE	MD [CI 95%]	RMSPE	MD [CI 95%]	RMSPE	MD [CI 95%]
	0.1	0.5 [0.5; 0.6]	0.1	0.7 [0.6; 0.9]	0.1	0.3 [0.2; 0.3]	0.1	0.6 [0.5; 0.7]
Rot Y Skull in TGF	Inter		Intra					
			Exam 1		Exam 2		Exam 3	
	RMSPE	MD [CI 95%]	RMSPE	MD [CI 95%]	RMSPE	MD [CI 95%]	RMSPE	MD [CI 95%]
	0.1	0.1 [0.1; 0.2]	0.0	0.2 [0.2; 0.3]	0.0	0.1 [0.1; 0.1]	0.1	0.1 [0.1; 0.1]

3.2. Amplitudes of Movement

The principal components of the movements (higher than 1 degree for the rotations and higher than 1 mm for the translations) were used to calculate the associated mean and standard deviation (Table 5).

Table 5. Mean +/− standard deviation of the main rotations in degrees and the translations in millimeters of the jaw compared to the skull and the skull compared to the thorax around the *X*-axis, *Y*-axis and *Z*-axis, for the opening/closing, protrusion and full length laterotrusion motion cycle, in neutral, slouched and military positions.

Position	Neutral			Slouched			Military		
Opening/closing									
	Rot Z	Trans X	Trans Y	Rot Z	Trans X	Trans Y	Rot Z	Trans X	Trans Y
Jaw	−27.0+/−6.3	−13.7+/−4.2	−6.4+/−3	−26.9+/−6.4	−13.0+/−4.1	−6.6+/−3.2	−25.2+/−7.1	−11.9+/−5.3	−6.1+/−3.4
Skull	2.2+/−3.2	2+/−1.5	<1	1.9+/−3.1	1.7+/−1.7	<1	1.6+/−2.1	1.7+/−1.5	<1
Protrusion									
	Rot Z	Trans X		Rot Z	Trans X		Rot Z	Trans X	
Jaw	3.8+/−1.9	10.3+/−2.7		4.0+/−2.2	10.4+/−2.6		4.1+/−2	10.6+/−2.8	
Skull	<1	8.9+/−6.2		<1	8.1+/−5.7		<1	6.4+/−4.5	
Left laterotrusion full length									
	Rot Y	Trans Z		Rot Y	Trans Z		Rot Y	Trans Z	
Jaw	12.3+/−3.1	−5.8+/−2.9		12.5+/−3	−7.0+/−3.6		12.3+/−3.1	−5.9+/−2.8	
Skull	4.2+/−4.8	−1.5+/−2.0		3.1+/−2.7	−1.7+/−2.1		3.5+/−3.4	−1.6+/−1.6	
Right laterotrusion full length									
Jaw	−11.1+/−4.7	5.9+/−2.8		−11.3+/−4.6	7.1+/−3.5		−11.1+/−4.7	5.8+/−2.9	
Skull	−3.9+/−4.8	2.0+/−2.5		−2.8+/−2.7	2.2+/−2.6		−3.2+/−3.4	1.9+/−2.0	

During opening and closing of the mouth and for all positions combined, we measured the mean amplitudes of rotation of the jaw compared to the skull of −26.4° ± 6.6 in the sagittal plane, 12.9 mm ± 4.5 of translation along the *X*-axis and −6.4 mm ± 3.2 along the *Y*-axis. Also, in each position, the subjects' heads rotated in the opposite direction, i.e., they extended. The mean amplitudes of movement of the skull compared to the thorax for all positions combined were 1.9° ± 2.8 for rotation around the *Z*-axis, and 1.8 mm ± 1.6 for translation along the *X*-axis.

During the protrusion movement, the mean values of translation along the *X*-axis of the jaw in relation to the skull for all positions combined were 10.4 mm ± 2.7. The jaw also rotated around the *Z*-axis by 4.0° ± 2.0. With regard to the movements of the head in relation to the thorax during protrusion, a participation of 7.8 mm ± 1.6 for the translational component on the *X*-axis can be observed.

Concerning the laterotrusion movement, we chose to consider a full laterotrusion cycle, meaning a movement from the most lateral position on one side to the other side. Indeed, from a functional point of view, the laterotrusion movement solicits muscles which are active throughout the entire "laterotrusion full length", and not just from the centered position of the mandible. Therefore, during the recording, we asked the subjects to move first to the left, then to the right without closing their mouths between the 2 sides.

The results showed a sideways movement of the mandible with a lateral translation component along the *Z*-axis and an axial rotation component around the *Y*-axis.

For the left laterotrusion full length, mean amplitudes for all positions were of 12.4° ± 3.1 of rotation about the *Y*-axis, and −6.2 mm ± 3.1 of translation about the *Z*-axis. For the right laterotrusion full length, −11.2° ± 4.6 of rotation about the *Y*-axis, and 6.3 mm ± 3.1 of translation about the *Z*-axis.

With regard to the movements of the head in relation to the thorax during the left and right full-length laterotrusion, we observed a participation of 3.6° ± 3.6 and −3.3° ± 3.6, respectively, for the rotational component on the *Y*-axis; −1.6 mm ± 3.6 and 2.0 mm ± 2.4, respectively, for the translation along the *Z*-axis.

These results will be discussed and compared with the literature in Section 4.2.

3.3. Amplitudes for Different Head Positions

Q-Q plots were performed to verify the normal distribution of all the components of movement and for the three different positions. These graphs are available in the Supplementary Material section.

From the normality tests, data were extracted in order to perform comparisons of means using repeated-measures ANOVA for normally distributed data or the Friedman test for non-parametric data (Table 6).

Table 6. Repeated-measures ANOVA for normally distributed data or Friedman test for non-parametric data ◊: *p* values intra-subject by head position, *p* values inter-subject by gender.

	Jaw		**Skull**	
	Opening–closing motion			
	p Head position	p Gender	p Head position	p Gender
Rot Z	0.233	0.406	0.549 ◊	/
Trans X	0.064	0.720	0.702	0.329
Trans Y	0.382	0.642	/	/
	Laterotrusion			
Rot Y	0.476	0.762	0.353 ◊	/
Trans Z	0.111	0.221	0.567 ◊	/
	Protrusion			
Trans X	0.826	0.648	0.779 ◊	/
Rot Z	0.715	0.633	/	/

The average amplitudes of movement of the jaw compared to the skull and the skull compared to the thorax, for the three different head positions, were not significantly different. Similarly, no significant gender difference was found.

3.4. Power Estimation of the Sample Size

To verify whether the absence of a significant difference between the means according to position is a true non-difference, in other words, whether there is a type II or β risk of

not detecting a difference when one actually exists, we calculated the power of our sample size (Table 7) using Cohen's f3 effect size test [32].

Table 7. Power estimation of the sample size of 0.692, for an error of type I or $\alpha = 0.2$, 12 subjects, 3 positions examined, maximum amplitude difference observed 2.5° +/− 3.5 for the rotation of the jaw around the *Z*-axis during the opening of the mouth.

Type I Error α	Number of Subjects	Number of Groups	Maximum Difference Between Two Groups	Within Group Standard Deviation	Power
0.2	12	3	2.5	3.5	0.692

From the power estimation of our sample size ($\beta = 0.692$), we can conclude that the power of the data is lower than the original planned value of 0.8, considered a standard threshold in many scientific fields.

3.5. Head and Jaw Coordination

The correlation between maximum amplitudes for the jaw compared to the skull and the skull compared to the thorax showed clear dependency between these two variables (Table 8).

Table 8. Relationship between maximum amplitude of the jaw in relation to the skull and the skull in relation to the thorax: coefficient of determination (R2).

Opening/Closing Rot Z	Laterotrusion Rot Y	Protrusion Trans X
0.913	0.958	0.874

Table 9 shows the percentages of the amplitude of skull motion compared to the jaw, for the same components of motion.

Table 9. Mean percentage (%) of the amplitudes of the skull compared to the amplitudes of the jaw.

Opening–closing	Rot Z	Mean	% skull
	Jaw	−26.4	
	Skull	1.9	7.2
Laterotrusion	Rot Y	Mean	% skull
	Jaw	12.3	
	Skull	3.6	29.2
Protrusion	Trans X	Mean	% skull
	Jaw	10.4	
	Skull	5.5	52.8

The importance of the skull contribution was, in decreasing order, 52.8% for the translation on *X*-axis during protrusion, 29.2% to the rotation around *Y*-axis during laterotrusion, and 7.2% to the rotation around *Z*-axis during the opening motion (this rotation of the skull is towards extension—hence its positive sign—and not flexion, as it is the case for the jaw).

In Figure 5, steady-state plots (SSPs) are shown. They appear as flattened rings with positive or negative trends, depending on the axis and the segment (head or jaw). For the opening–closing motion, the jaw rotates negatively around the *Z*-axis (the mouth opens) while the head extends and thus rotates positively (2 to 3°) around the same axis.

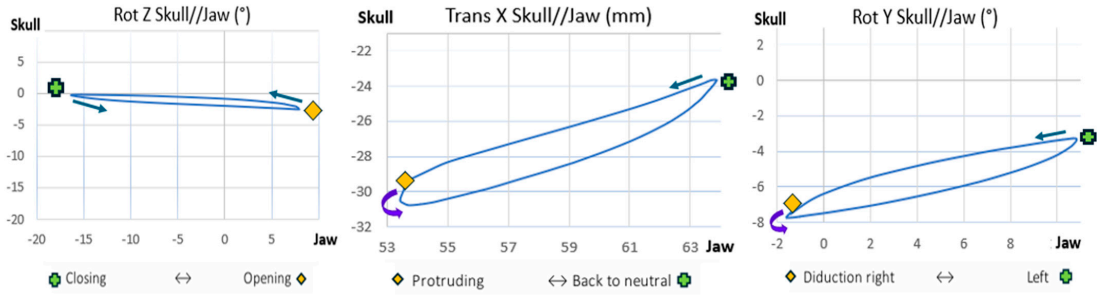


Figure 5. (**a**): Amplitude of rotation in degrees of the skull relative to the jaw around the Z-axis during mouth opening and closing movements. ◆ Start of the opening movement; ✤ start of the closing movement; (**b**): Amplitude of translation of the skull relative to the jaw on the X-axis during pro-trusion and retrusion movements. ◆ Start of the protrusion movement; ✤ start of the retrusion movement; (**c**): Amplitude of rotation of the skull relative to the jaw around the Y-axis during laterotrusion movements. ◆ Start of the laterotrusion movement to the left; ✤ start of the laterotrusion movement to the right. The arrows indicate the direction of movement.

During protrusion motion, translation on the *X*-axis is positive for both segments (10 mm for the jaw and 7 mm for the head).

For the laterotrusion, the jaw and the head rotate around the *Y*-axis positively (11 to 12° and 3° respectively), i.e., they both turn to the left during left laterotrusion. The SSP also shows a ring spread out almost exclusively over positive abscissa values, demonstrating a much greater amplitude while laterotrusion towards the left than towards the right.

In Figure 6, the normalized amplitudes of movement of the jaw and skull between 0 and 1 during the motion cycle show that, whatever the position or movement, the jaw always reached its maximum amplitude before the head.

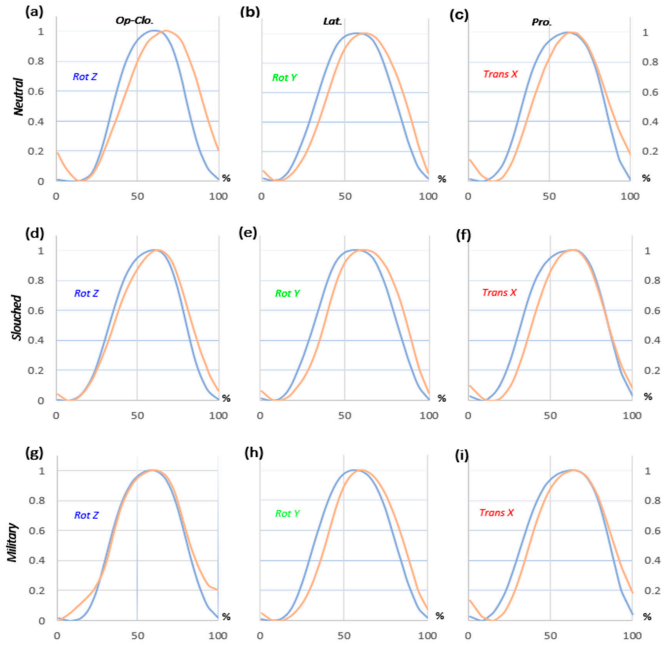


Figure 6. Graphs of the normalized amplitudes (between 0 and 1) of the jaw (—) and the skull (—). Amplitude of rotation around the *Z*-axis during the mouth opening–closing motion cycle for the neutral (**a**), slouched (**d**) and military positions (**g**). Amplitude of rotation around *Y*-axis during the laterotrusion motion cycle for the neutral (**b**), slouched (**e**) and military positions (**h**). Amplitude of translations on *X*-axis during the protrusion motion cycle for the neutral (**c**), slouched (**f**) and military positions (**i**).

4. Discussion

4.1. Reliability of the Protocol

The precision analysis of the ALs placement (taped or the mandible cluster) and of the ALs palpated with the A-Palp highlighted the good intra-examiner repeatability and inter-examiner reproducibility (Table 3). In the context of in vivo palpation, these repeatability values are similar or better compared to those found in other AL-based motion analysis studies [20,33,34].

For inter-examiner reproducibility, the most difficult AL to palpate accurately was the spinous processes of TH2 (Inter-examiner MD: −20.7 mm) because it is generally covered by soft tissue or it has a large surface. Consequently, particular attention must be paid in the future to the palpation definitions and technique and its careful reproduction, or to choosing other close ALs that would be more easily palpated and therefore more reproducible.

Greater precision of markers palpated with the A-Palp was observed compared with glued markers. This is explained by the fact that palpation with the A-palp of subcutaneous ALs is recorded and that the markers thus located do not move subsequently during movements in relation to the other markers. Nevertheless, the examiner must be trained in palpation in order to always perform it in the same way in an experimental or clinical context. The glued markers were able to move with the skin during the subject's movements.

Inter- and intra-examiner RMSPE for the skull and the jaw movements demonstrated a sufficiently small propagation of the precision error for a motion analysis study (Table 4).

These results are consistent with our effort to quantify the reliability of our measurements (location of anatomical landmarks and range of motion) and can be considered satisfactory.

4.2. Amplitudes of Head and Jaw Movements

The amplitudes of the opening–closing movement (Table 5) are in line with those found in the literature [35–37]. The subjects' head extensions measured in our study were lower than those reported by Prodoehl et al. (2022): 7.9° ± 1.2. This dissimilarity could be explained by a different measurement protocol (4 optoelectronic cameras, 3 taped clusters) [16].

Also, we found values of 1.8 mm ± 1.6 for head translation along the TGF *X*-axis, showing that the head moves slightly forward when the subject opens the mouth.

These amplitudes of rotation and translation of the head in relation to the thorax may seem small, but they show their simultaneity with the movements of the jaw. Unintentionally, the head rotates backwards when the jaw opens and returns when the jaw closes. The cause of these combined movements may lie in the greater submandibular space created by the head extension, allowing a wider mouth opening [38,39].

For the protrusion movement, our measurements correspond to the values reported in the literature [40]. The amplitude of translation along the *X*-axis indicated a significant displacement in the sagittal plane, which may result in a non-negligible mechanical stress on the joint. However, this translation remained less than that observed during mouth opening.

The rotation of the jaw around the *Z*-axis observed during the protrusion allows the lower dental arch to move around the upper one and forward.

Concerning the laterotrusion movements, our results correspond to those found in the literature: Shu et al. [36] reported 4 to 8 mm of condylar displacement in the frontal plane for five healthy subjects and from an optical motion-track system recording. Del Palomar et al. [41] presented 10.69 mm of condylar displacement towards the right during the right laterotrusion motion of one healthy subject and the same motion recording methodology. Bescond et al. [35] reported for the left laterotrusion, full length 10.7° ± 2.1 for the rotation around the *Y*-axis, and −9.4 mm ± 1.3 for the translation on the *Z*-axis.

From a functional point of view, it is the lateral and medial pterygoid muscles that pull the mandible from side to side during laterotrusion movements. We could therefore hypothesize that this asymmetry in amplitude is a consequence of their different actions.

4.3. Amplitudes of the Jaw for Different Head Positions

One of the objectives of this study was to investigate the influence of head position on mandibular movements by placing the subjects in a slouched or military position. The slouched position could have led to an extension of the head in relation to the thorax, while the military position could have led to a flexion of the head. However, we did not force the subjects to remain in these positions, nor did we measure the changes in the cervical spine. The result showed no significant difference (Table 6). Given the statistical insignificance of the results, it was not necessary to perform a Tukey post hoc test.

Considering the small size of our sample, we conducted a power analysis estimation of the type II or $\beta = 0.692$. Usually set at a minimum value of 0.8 in clinical research, this meant that our sample was not big enough to allow our statistical tests to be sufficiently powerful to detect a real effect of the subjects' position on the amplitude of their jaw.

A previous study by Taghizadeh [42] reported a significant decrease in the antero-posterior amplitude of one mandibular condyle during movements of maximum mouth opening for subjects with a severe forward head posture, i.e., with a craniocervical angle between 40 and 44°. Greater cervical lordosis, according to the authors, is likely to create tensions on the suprahyoid and infrahyoid muscles, as well as on the mandible, and prevent the condyle from advancing. No changes in the amplitude of the mandible in the slouched position, which a priori leads to greater cervical lordosis, were found. However, our subjects were placed in this position artificially and not due to pathological conditions. Also, Taghizadeh's [42] measurements were made with an ultrasound device and on a single condyle. He did not specify whether the amplitude of rotation in the sagittal plane or the interincisal distance were modified.

Prodoehl [16] showed that body position influences the maximum opening amplitude of the mouth: the opening in the slouched position is smaller than in the military position, which is smaller than in the neutral position. However, these different positions do not influence the amplitude of head movements.

Apart from the small size of our population, our results can also be explained by the position in which we placed our subjects. We asked them not to move their upper body and remain still once seated, but their position was neither standardized nor constrained. They were free to 'break' out of the military or slouched position as they wished, sitting on a stool without a backrest or headrest.

4.4. Coordinated Movements of the Head and Jaw

The contribution of the cervical spine during TMJ movements is quantified in Table 9: head motions for the same movement components represent 52.8% during protrusion, 29.2% during laterotrusion and 7.2% during mouth opening, the latter in the opposite direction to the jaw. The head therefore systematically accompanies the movements of the jaw, even during mastication and despite much smaller amplitudes of movement: Kohno (38) found that the range of movement of the head was 10% of that of the jaw during rhythmic mastication.

The origin of the simultaneous movements of the head during protrusion and laterotrusion of the mandible is not clear: protrusion and laterotrusion are not functional movements that we perform involuntarily on a daily basis, unlike mouth opening and mastication. It is therefore difficult to deduce a functional interpretation from them. Perhaps

this was the result of the subjects performing the movements to the best of their ability, as requested by the examiner.

Coefficients of determination R2 between the amplitude of the mandible and of the skull demonstrated a strong relationship between the two segments (Table 8).

Steady-state plots (Figure 5) enabled us to observe the positive or negative trend in the simultaneous amplitudes of the segments on an axis during the movement cycle. The flat ring shapes, which are a priori normal, i.e., a reflection of the amplitudes of asymptomatic subjects, could be used in routine movement analysis to observe their deformation or displacement relative to the axis in the case of a mobility defect.

Finally, the normalized amplitude graphs (Figure 6) showed the offset between the moment when the jaw reached its maximum amplitude along an axis and the moment when the head also reached it. It would appear that the head follows the jaw systematically, whatever the movement studied.

The observations concerning temporal coordination between the head and the jaw differ according to the authors: Eriksson [15] and Zafar [14] observed that the head preceded the jaw during rhythmic mouth-opening movements. But the start of the movement was imposed by a metronome, which may have induced anticipation on the part of the subjects. Torisu [43] in contrast, observed that the jaw always moved before the head during rapid but free movements.

4.5. Limitation

Our study, as already mentioned, has methodological limitations, including the small size of our sample (n = 12) and the lack of standardized head positions relative to the thorax during mandibular movements. Therefore, the non-significant results obtained in the statistical tests of mean differences should be interpreted with great caution, as demonstrated by the power analysis estimation.

Nevertheless, we consider the accuracy of our protocol to be methodologically valid, as it focused on the location and movement of 20 markers during a very large number of movements (3 series of 10 movements in 3 different positions).

4.6. Use of the Protocol During Clinical Evaluation

In light of the results of the reproducibility, repeatability and error propagation study, the protocol has proven its robustness. The time required for palpation, placement of the ALs and recording of movements does not exceed half an hour. Taking impressions of the lower teeth and fabricating the mandibular splint requires a prior appointment and a manufacturing lead time; however, the custom-made splint can be reused by the subject for treatment evaluation purposes, for example, to objectively assess a change in mandibular or cephalic kinematics.

In the field of TMD, clinical guidelines have progressed towards, among other things, the need for in vivo kinematic assessment tools including the cervical spine, in order to compare normal vs. pathological cases and to improve patient care [44,45]. Few authors have developed motion analysis protocols combining head with mandibular kinematics for clinical evaluation purposes (14), thereby highlighting the natural biological jaw–head movement. We wish to adopt the same approach to clinical use.

Therefore, sample size estimation, improving palpation techniques, and standardizing the position of subjects represent the next steps in order to complete our study.

5. Conclusions

The aim of this study was to measure the amplitudes of simultaneous movements of the jaw in relation to the skull and of the skull in relation to the thorax, during mouth

opening and closing movements, laterotrusion and protrusion, and for different head positions, in healthy subjects.

The protocol for AL palpation and marker placement proved highly accurate, as did the amplitudes measured.

The different positions taken by the subjects during the execution of the movements did not significantly influence the amplitudes of the mandible in relation to the skull, probably because the position of the subjects was not fixed and the sample size was too small.

Our measurements revealed the substantial participation of head movements in those of the jaw, for all movements and in all positions. These results are consistent with the literature. They highlight the need to include data on the coordination of these two segments during clinical analysis.

Supplementary Materials: The following supporting information can be downloaded at https://www.mdpi.com/article/10.3390/biomechanics6010011/s1, Figure S1: Opening and closing movement of the mouth. Q-Q plots for (A) the rotation around the *Z*-axis of the jaw in neutral, slouched and military positions; (B) the translation along the *X*-axis of the jaw in neutral, slouched and military positions; (C) the translation along the *Y*-axis of the jaw in neutral, slouched and military positions; (D) the rotation around the *Z*-axis of the skull in neutral, slouched and military positions; (E) the translation along the *X*-axis of the skull in neutral, slouched and military positions.

Author Contributions: Conceptualization, G.B.; methodology, G.B. and V.F.; Software, J.A.N., F.M. and S.V.S.J.; investigation, G.B. and C.D.P.; data curation, G.B. and C.D.P.; writing—original draft preparation, G.B.; writing—review and editing, S.V.S.J. All authors have read and agreed to the published version of the manuscript.

Funding: This research received no external funding.

Institutional Review Board Statement: The study was conducted in accordance with the Declaration of Helsinki and approved by the Board of Ethics of the ULB (No. SRB2023/356, date of approval: July 2023).

Informed Consent Statement: Informed consent was obtained from all subjects involved in the study.

Data Availability Statement: The original contributions presented in this study are included in the article/Supplementary Material. Further inquiries can be directed to the corresponding author.

Conflicts of Interest: The authors declare no conflicts of interest.

Abbreviations

The following abbreviations are used in this manuscript:

AFs	Anatomical frames
ALs	Anatomical landmarks
CCDI	Craniocervical dysfunction index
ISB	International society of biomechanics
JGF	Jaw global frame
LJA	Left jaw angle
LAT	Left acromial tip
LMP	Left mastoid process
MP	Mental protuberance

GL	Glabella
JN	Jugular notch
RDC-TMD	Research and diagnostic criteria for temporomandibular disorder
RJA	Right jaw angle
RAT	Right acromial tip
RMP	Right mastoid process
SGF	Skull global frame
TGF	Thorax global frame
TH2	Spinous process of Th2

References

1. Siu, W.; Shih, Y.; Lee, S.; Hsu, C.; Wei, M.; Wang, T.; Lin, H.; Lin, Y. Alterations in kinematics of temporomandibular joint associated with chronic neck pain. *J. Oral Rehabil.* **2022**, *49*, 860–871. [CrossRef] [PubMed]
2. Storm, C.; Wänman, A. Temporomandibular disorders, headaches, and cervical pain among females in a Sami population. *Acta Odontol. Scand.* **2006**, *64*, 319–325. [CrossRef] [PubMed]
3. Armijo-Olivo, S.; Magee, D. Cervical Musculoskeletal Impairments and Temporomandibular Disorders. *J. Oral Maxillofac. Res.* **2013**, *3*, e4. Available online: http://www.ejomr.org/JOMR/archives/2012/4/e4/v3n4e4ht.htm (accessed on 1 January 2025).
4. Mehta, R.; Keith, D. Temporomandibular Disorders in Adults. Available online: https://www-uptodate-com.ezproxy.ulb.ac.be/contents/temporomandibular-disorders-inadults?search=tmj&source=search_result&selectedTitle=1~94&usage_type=default&display_rank=1#H548815367(accessed on 13 November 2024).
5. Makofsky, H.W. The Effect of Head Posture on Muscle Contact Position: The Sliding Cranium Theory. *CRANIO®* **1989**, *7*, 286–292. [CrossRef] [PubMed]
6. Clauzade, M. Orthoposturodontie. *Actual. Odonto-Stomatol.* **2007**, *240*, 387–405. [CrossRef]
7. Borel, L.; Paya-Argoud, M.; Cheynet, F.; Raskin, A.; Le Gall, M.; Tardieu, C. Conséquences d'un changement drastique de la proprioception mandibulaire sur la posture après chirurgie orthognatique. *Neurophysiol. Clin.* **2015**, *45*, 401. [CrossRef]
8. Manfredini, D.; Castroflorio, T.; Perinetti, G.; Guarda-Nardini, L. Dental occlusion, body posture and temporomandibular disorders: Where we are now and where we are heading for: Occlusion, posture, and temporomandibular disorders. *J. Oral Rehabil.* **2012**, *39*, 463–471. [CrossRef]
9. Winnberg, A.; Pancherz, H.; Westesson, P.L. Head Posture and Hyo-Mandibular Function in Man. A Synchronized Electromyographic and Videofluorographic Study of the Open-Close-Clench Cycle. *Am. J. Orthod. Dentofac. Orthop.* **1988**, *94*, 393–404. [CrossRef]
10. Piovesan, E.J.; Kowacs, P.A.; Oshinsky, M.L. Convergence of Cervical and Trigeminal Sensory Afferents. *Curr. Pain Headache Rep.* **2003**, *7*, 377–383. [CrossRef]
11. Fougeront, N.; Fleiter, B. Temporomandibular Disorder and Comorbid Neck Pain: Facts and Hypotheses Regarding Pain-Induced and Rehabilitation-Induced Motor Activity Changes. *Can. J. Physiol. Pharmacol.* **2018**, *96*, 1051–1059. [CrossRef]
12. Goldstein, D.F.; Kraus, S.L.; Willams, W.B.; Glasheen-Wray, M. Influence of cervical posture on mandibular movement. *J. Prosthet. Dent.* **1984**, *52*, 421–426. [CrossRef]
13. Visscher, C.M.; Huddleston Slater, J.J.R.; Lobbezoo, F.; Naeije, M. Kinematics of the human mandible for different head postures. *J. Oral Rehabil.* **2000**, *27*, 299–305. [CrossRef] [PubMed]
14. Zafar, H.; Nordh, E.; Eriksson, P.O. Temporal coordination between mandibular and head–neck movements during jaw opening–closing tasks in man. *Arch. Oral Biol.* **2000**, *45*, 675–682. [CrossRef] [PubMed]
15. Eriksson, P.O.; Häggman-Henrikson, B.; Nordh, E.; Zafar, H. Co-ordinated Mandibular and Head-Neck Movements during Rhythmic Jaw Activities in Man. *J. Dent. Res.* **2000**, *79*, 1378–1384. [CrossRef] [PubMed]
16. Prodoehl, J.; Thomas, P.; Krzak, J.J.; Hanke, T.; Tojanic, J.; Thomas, J. Effect of Starting Posture on Three-Dimensional Jaw and Head Movement. *J. Oral Maxillofac. Res.* **2022**, *13*, e1. Available online: http://www.ejomr.org/JOMR/archives/2022/1/e4/v13n1e4ht.htm(accessed on 26 May 2023). [CrossRef]
17. Nilsson, E.; Grip, H.; Österlund, C. Accuracy and reliability for estimating jaw functional range of motion. *Gait Posture* **2024**, *113*, 280–286. [CrossRef]
18. Schiffman, E.; Ohrbach, R.; Truelove, E.; Look, J.; Anderson, G.; Goulet, J.P.; List, T.; Svensson, P.; Gonzalez, Y.; Lobbezoo, F.; et al. Diagnostic Criteria for Temporomandibular Disorders (DC/TMD) for clinical and research applications: Recommendations of the international RDC/TMD consortium network and orofacial pain special interest group. *J. Oral. Facial Pain Headache* **2014**, *28*, 6–27. [CrossRef]
19. Wallace, C.; Klineberg, I.J. Management of craniomandibular disorders. Part 1: A craniocervical dysfunction index. *J. Orofac. Pain.* **1993**, *7*, 83–88.

20. Salvia, P.; Van Sint Jan, S.; Crouan, A.; Vanderkelen, L.; Moiseev, F.; Sholukha, V. Precision of shoulder anatomical landmark calibration by two approaches: A cast-like protocol and a new anatomical palpator method. *Gait Posture* **2009**, *29*, 587–591. [CrossRef]
21. Van Sint Jan, S. *Color Atlas of Skeletal Landmark Definitions: Guidelines for Reproducible Manual and Virtual Palpations*; Churchill Livingstone Elsevier: Edinburgh, UK, 2007.
22. Viceconti, M.; Taddei, F.; Montanari, L.; Testi, D.; Leardini, A.; Clapworthy, G.; Van Sint Jan, S. Multimod Data Manager: A tool for data fusion. *Comput. Methods Programs Biomed.* **2007**, *87*, 148–159. [CrossRef]
23. Wu, G.; Cavanagh, P. ISB recommendation for standardization in the reporting of kinematic data. *J. Biomech.* **1995**, *28*, 1257–1261. [CrossRef]
24. Cappozzo, A.; Catani, F.; Della Croce, U.; Leardini, A. Position and Orientation in Space of Bones during Movement: Anatomical Frame Definition and Determination. *Clin. Biomech.* **1995**, *10*, 171–178. [CrossRef]
25. Beyer, B.; Feipel, V.; Sholukha, V.; Chèze, L.; Van Sint Jan, S. In-vivo analysis of sternal angle, sternal and sternocostal kinematics in supine humans during breathing. *J. Biomech.* **2017**, *64*, 32–40. [CrossRef] [PubMed]
26. Mahieu, C.; Salvia, P.; Beyer, B.; Rooze, M.; Feipel, V.; Van Sint Jan, S. Metatarsal arch deformation and forefoot kinematics during gait in asymptomatic subjects. *Int. Biomech.* **2019**, *6*, 75–84. [CrossRef] [PubMed]
27. Snoeck, O.; Coupier, J.; Beyer, B.; Salvia, P.; Lefèvre, P.; Van Sint Jan, S.; Rooze, M.; Feipel, V. The biomechanical role of the lacertus fibrosus of the biceps brachii Muscle. *Surg. Radiol. Anat. Engl. Ed.* **2021**, *43*, 1587–1594. [CrossRef] [PubMed]
28. Woltring, H.J. A Fortran package for generalized, cross-validatory spline smoothing and differentiation. *Adv. Eng. Softw.* **1986**, *8*, 104–113. [CrossRef]
29. D'Amico, M.; Ferrigno, G. Comparison between the more recent techniques for smoothing and derivative assessment in biomechanics. *Med. Biol. Eng. Comput.* **1992**, *30*, 193–204. [CrossRef]
30. Vaughan, C.L. Smoothing and differentiation of displacement-time data: An application of splines and digital filtering. *Int. J. Bio-Med. Comput.* **1982**, *13*, 375–386. [CrossRef]
31. Portney, L.; Gross Watkins, M.P. *Foundations of Clinical Research: Applications to Practice*, 2nd ed.; Prentice Hall: Upper Saddle River, NJ, USA, 2000.
32. Cohen, J. *Statistical Power Analysis for the Behavioral Sciences*, 2nd ed.; Lawrence Erlbaum Associates, Pubishers: London, UK, 1988; pp. 276–279+550. ISBN 0-8058-0283-5. Available online: https://www.StatsToDo.com/MakeTable.php (accessed on 17 December 2025).
33. Calixtre, L.B.; Nakagawa, T.H.; Alburquerque-Sendín, F.; da Silva Grüninger, B.L.; de Sena Rosa, L.R.; Oliveira, A.B. Inter- and intra-rater reliability of 3D kinematics during maximum mouth opening of asymptomatic subjects. *J. Biomech.* **2017**, *64*, 245–252. [CrossRef]
34. Van Keirsbilck, M.M. Reproductibility of the 3D Temporo-Mandibular Joint Kinematics. Master's Thesis, Université Libre de Bruxelles, Bruxelles, Belgium, 2011. Available online: http://homepages.ulb.ac.be/ labo (accessed on 15 February 2024).
35. Bescond, G.; Gales, M.; Glineur, R.; Sholukha, V.; Louryan, S.; Van Sint Jan, S. Complete 3D Kinematics Parameters of the Temporo-Mandibular Joints Using in Vivo Data Fusion. *IRBM* **2023**, *44*, 100804. [CrossRef]
36. Shu, J.; Ma, H.; Jia, L.; Fang, H.; Chong, D.Y.R.; Zheng, T.; Yao, J.; Liu, Z. Biomechanical behaviour of temporomandibular joints during opening and closing of the mouth: A 3D finite element analysis. *Int. J. Numer. Methods Biomed. Eng.* Available from. **2020**, *36*, e3373. Available online: https://onlinelibrary.wiley.com/doi/10.1002/cnm.3373 (accessed on 18 November 2021). [CrossRef]
37. Travers, K.H.; Buschang, P.H.; Hayasaki, H.; Throckmorton, G.S. Associations between incisor and mandibular condylar movements during maximum mouth opening in humans. *Arch. Oral Biol.* **2000**, *45*, 267–275. [CrossRef]
38. Kohno, S.; Matsuyama, T.; Medina, R.U.; Arai, Y. Functional-rhythmical coupling of head and mandibular movements. *J. Oral Rehabil.* **2001**, *28*, 161–167. [CrossRef]
39. Koolstra, J.H.; van Eijden, T.M.G.J. Functional significance of the coupling between head and jaw movements. *J. Biomech.* **2004**, *37*, 1387–1392. [CrossRef] [PubMed]
40. Baeyens, J.P.; Gilomen, H.; Erdmann, B.; Clijsen, R.; Cabri, J.; Vissers, D. In vivo measurement of the 3D kinematics of the temporomandibular joint using miniaturized electromagnetic trackers: Technical report. *Med. Biol. Eng. Comput.* **2013**, *51*, 479–484. [CrossRef] [PubMed]
41. Del Palomar Ap Doblare, M. Finite element analysis of the temporomandibular joint during lateral excursions of the mandible. *J. Biomech.* **2006**, *39*, 2153–2163. [CrossRef] [PubMed]
42. Taghizadeh Delkhoush, C.; Purzolfi, M.; Mirmohammadkhani, M.; Sadollahi, H.; Tavangar, S. The linear intra-articular motions of the temporomandibular joint in individuals with severe forward head posture: A cross-sectional study. *Musculoskelet. Sci. Pract.* **2024**, *70*, 102908. [CrossRef]
43. Torisu, T.; Yamabe, Y.; Hashimoto, N.; Yoshimatsu, T.; Fujii, H. Head movement properties during voluntary rapid jaw movement in humans. *J. Oral Rehabil.* **2001**, *28*, 1144–1152. [CrossRef]

44. Almarza, A.J.; Mercuri, L.G.; Arzi, B.; Gallo, L.M.; Granquist, E.; Kapila, S.; Detamore, M.S. Temporomandibular Joint Bioengineering Conference: Working Together Toward Improving Clinical Outcomes. *J. Biomech. Eng.* **2019**, *142*, 020801. Available online: https://asmedigitalcollection.asme.org/biomechanical/article-abstract/142/2/020801/955405/Temporomandibular-Joint-Bioengineering-Conference (accessed on 16 June 2025).
45. Detamore, M.S.; Athanasiou, K.A.; Mao, J. A Call to Action for Bioengineers and Dental Professionals: Directives for the Future of TMJ Bioengineering. *Ann. Biomed. Eng.* **2007**, *35*, 1301–1311. [CrossRef]

Disclaimer/Publisher's Note: The statements, opinions and data contained in all publications are solely those of the individual author(s) and contributor(s) and not of MDPI and/or the editor(s). MDPI and/or the editor(s) disclaim responsibility for any injury to people or property resulting from any ideas, methods, instructions or products referred to in the content.